

Figure S1: Additional examples of the flux estimation by ogive optimization and EddyPro (with and without spectral corrections after *Moncrieff et al.* (1997, 2004)). Local time, average horizontal wind speed (U), wind direction, air temperature (T_{air}) and quality flag (QC) are given in the lower right of each panel. a: Nighttime release during the growing season showing acceptable agreement between the methods. b: Growing season uptake when both methods agree. c: Small release during strong wind in wintertime. After stabilization of the ogives in the mid frequency range, contributions of the lowest frequencies implausibly suggest CO_2 uptake in conventional flux estimates. d: Similar situation during calm conditions in October.

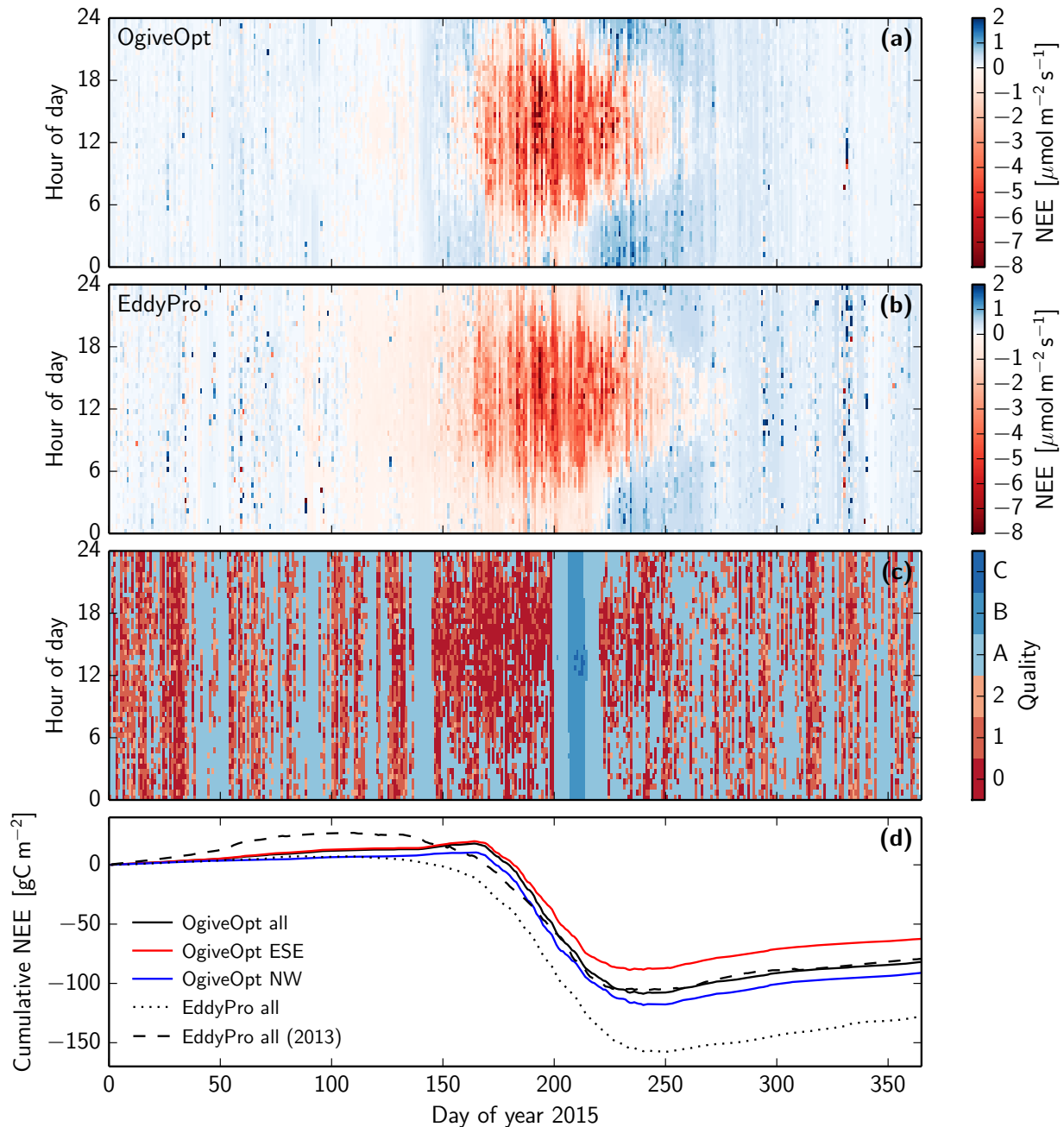


Figure S2: Gap-filled NEE fluxes and quality flags. a: Fingerprint plot of ogive optimization results of 2015. b: Corresponding EddyPro results. c: Corresponding quality flags based on *Foken and Wichura* (1996) and *Reichstein et al.* (2005). d: Cumulative sums based on all measurements, and separately gap-filled for the two footprints. The EddyPro results from 2013 are based on raw CO_2 measurements as wet molar densities, which renders them less certain than the 2015 data and prevented flux calculations using ogive optimization.

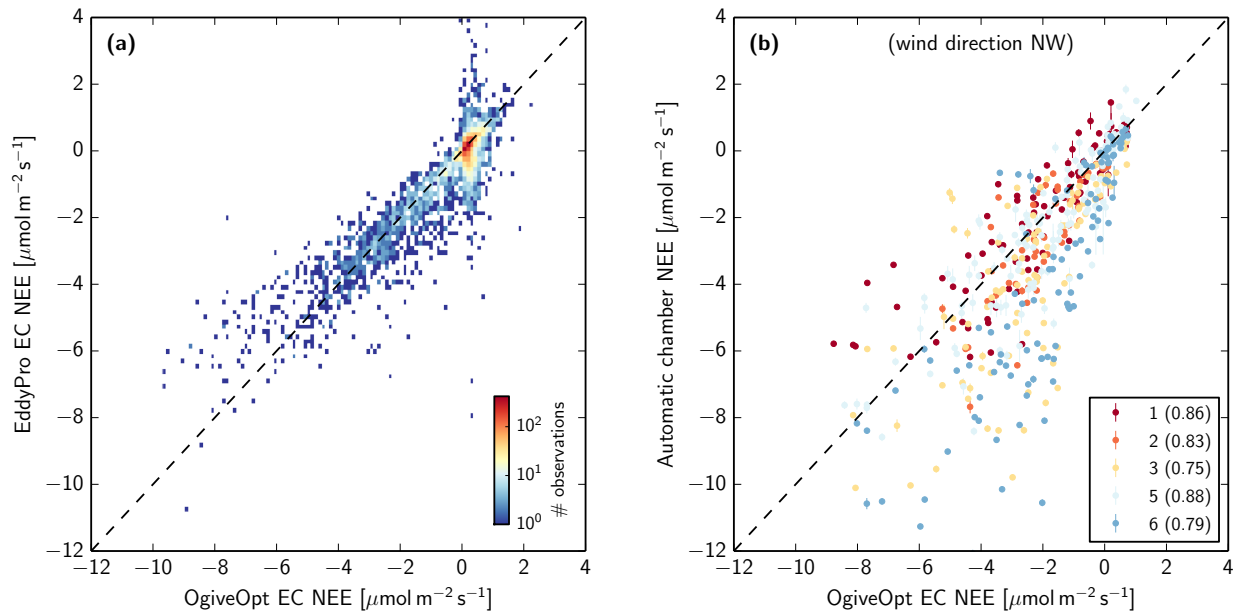


Figure S3: Comparison of ogive optimization fluxes to other methods. a: Histogram of conventional EC fluxes calculated by EddyPro (correlation $r=0.88$). b: Five individual automatic flux chambers located in the NW footprint (chamber 4 was not operational). Numbers in parentheses denote correlation coefficients. Corresponding p-values are all smaller than 10^{-12} .

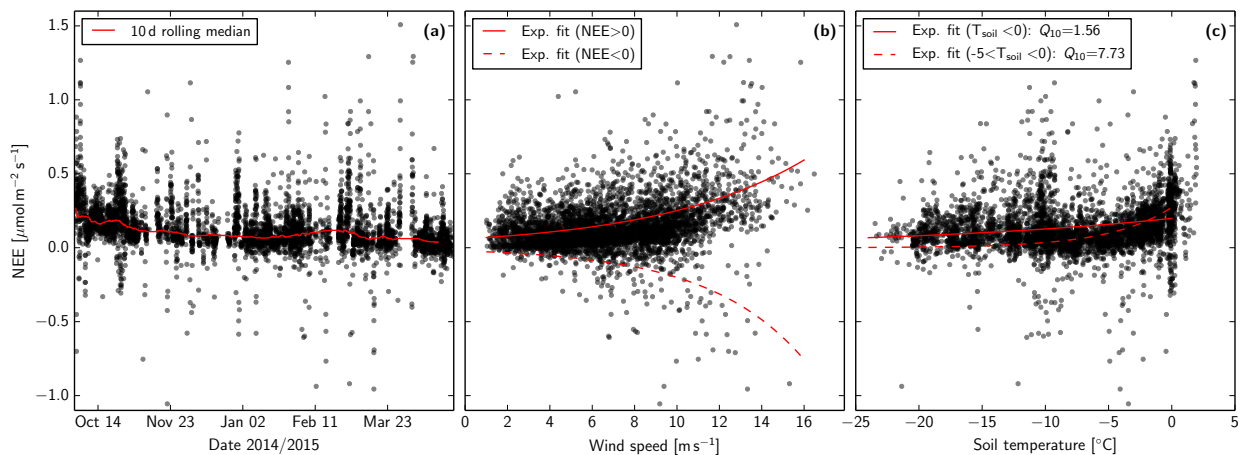


Figure S4: NEE results of ogive optimization between 1 October 2014 and 1 May 2015. a: Time series. b: Relation with wind speed. c: Relation with soil temperature (10 cm depth).

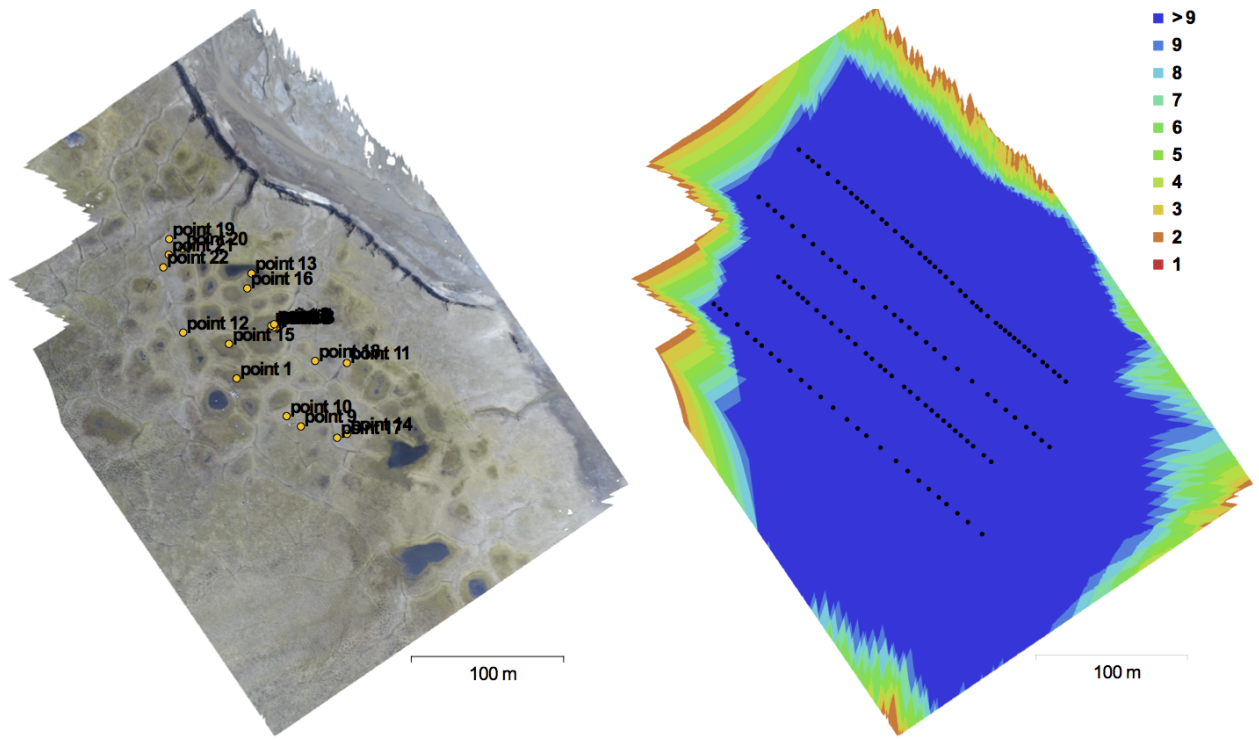


Figure S5: Details of the topographical survey. Left: Ground control points. Right: Camera locations and image overlap.



Figure S6: Photos of the environment and instrumentation on 19 August 2013 (left) and 7 October 2015 (right).

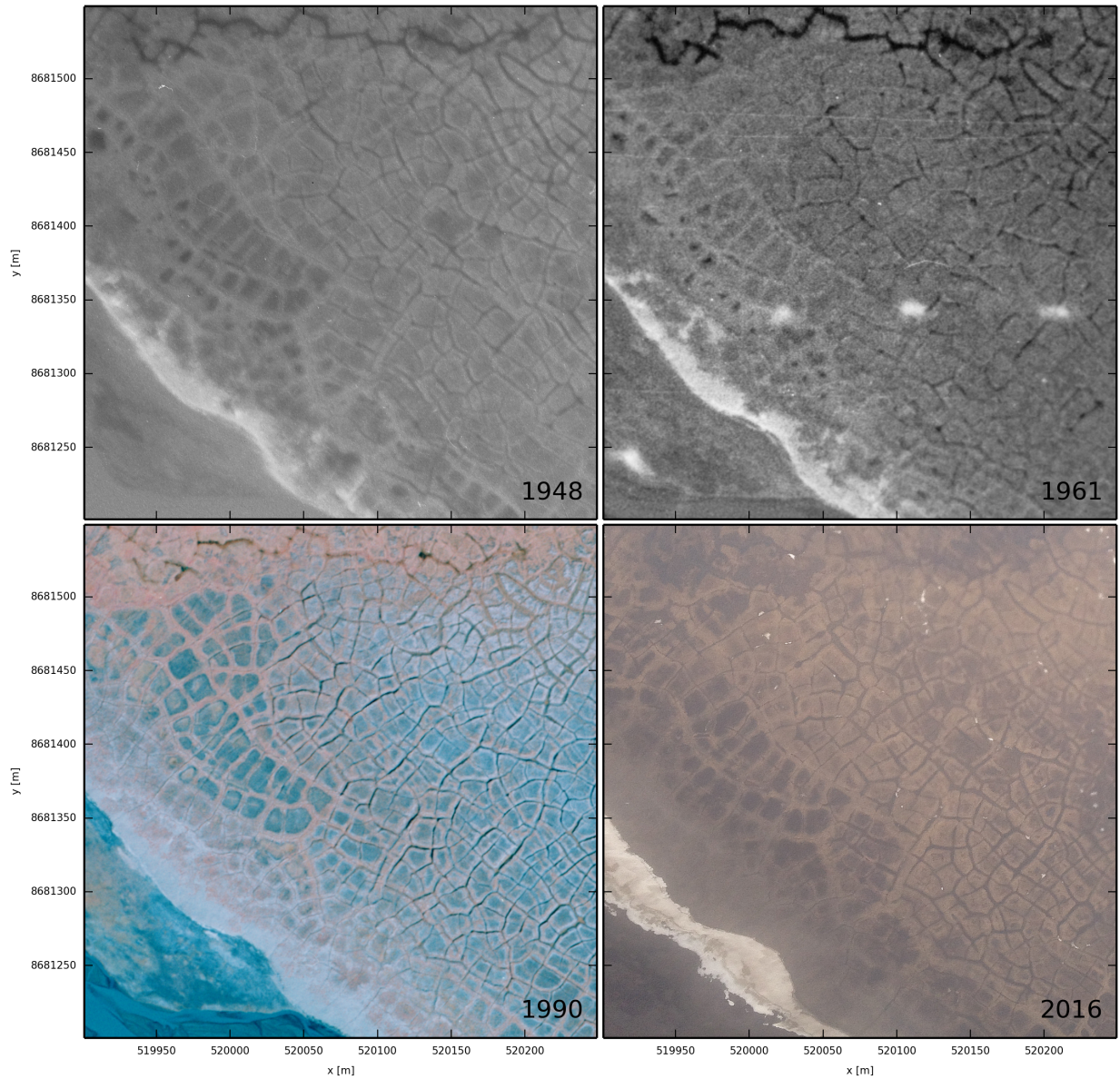


Figure S7: Time series of aerial images from the northern side of Adventdalen, 2.4 km away from the measurement site. Both low-centered and high-centered polygons show little signs of differential ground subsidence, which would indicate ice-wedge degradation. Historical photographs were provided by the Norwegian Polar Institute (reference numbers S48-5181, S61-3301 and S90-5273). The images from 1948 and 1961 were taken on panchromatic films, and the image from 1990 is a near infra-red (false color) photography.

References

- Foken, T., and B. Wichura (1996), Tools for quality assessment of surface-based flux measurements, *Agricultural and forest meteorology*, 78(1), 83–105.
- Moncrieff, J., R. Clement, J. Finnigan, and T. Meyers (2004), Averaging, detrending, and filtering of eddy covariance time series, in *Handbook of micrometeorology*, pp. 7–31, Springer.
- Moncrieff, J. B., et al. (1997), A system to measure surface fluxes of momentum, sensible heat, water vapour and carbon dioxide, *Journal of Hydrology*, 188, 589–611.
- Reichstein, M., et al. (2005), On the separation of net ecosystem exchange into assimilation and ecosystem respiration: review and improved algorithm, *Global Change Biology*, 11(9), 1424–1439.